Glycobiology, 2025, **35**, cwaf013
https://doi.org/10.1093/glycob/cwaf013
Advance access publication date 5 March 2025
Original Article

RCL glycosylation of serum corticosteroid-binding globulin: implications in cortisol delivery and septic shock

Anastasia Chernykh[1], Zeynep Sumer-Bayraktar[1], Jessica H. Lee[2,3], Emily J. Meyer[2,3], David J. Torpy[2,3] and Morten Thaysen-Andersen[1,4,*]

[1]School of Natural Sciences, Macquarie University, 4 Wally's Walk, Macquarie Park, 2109, New South Wales, Australia, [2]Department of Medicine, University of Adelaide, Corner of George Street and North Terrace, Adelaide, 5000, South Australia, Australia, [3]Endocrine and Metabolic Unit, Royal Adelaide Hospital, Port Road, Adelaide, 5000, South Australia, Australia, [4]Institute for Glyco-core Research (iGCORE), Nagoya University, Furocho, Chikusa Ward, Nagoya, 464-8601, Aichi, Japan

*Corresponding author. School of Natural Sciences, Faculty of Science and Engineering, Macquarie University, Building 4WW, Office 333, Macquarie Park, 2109, New South Wales, Australia. Email: morten.andersen@mq.edu.au

Corticosteroid-binding globulin (CBG) is a serum glycoprotein that binds and delivers anti-inflammatory cortisol to inflammatory sites through neutrophil elastase-mediated proteolysis of an exposed reactive centre loop (RCL) on CBG. Timely and tissue-specific delivery of cortisol is critical to alleviate inflammation including in life-threatening septic shock conditions. Herein, we firstly summarise our recently published report of functional RCL *O*- and *N*-glycosylation events of serum CBG (*Chernykh, J Biol Chem, 2023*). A key finding of that published work was the LC–MS/MS-based discovery of RCL *O*-glycans at Thr342 and Thr345 of serum CBG and their inhibitory roles in neutrophil elastase-mediated RCL proteolysis. While these observations are of significance as they implicate RCL *O*-glycosylation as a potential regulator of cortisol delivery, the link to septic shock remains unexplored. To this end, we used a similar LC–MS/MS approach to profile the RCL *O*-glycosylation of CBG purified from serum of twelve septic shock patients. Serum CBG from all patients exhibited RCL *O*-glycosylation comprising (di)sialyl T ($NeuAc_{1\text{-}2}Gal_1GalNAc_1$) core 1-type *O*-glycan structures decorating exclusively the Thr342 site. Importantly, relative to less severe cases, individuals presenting with the most severe illness displayed elevated RCL *O*-glycosylation upon ICU admission, suggesting a previously unknown link to septic shock severity. Overall, we have elucidated the coordinated RCL *N*- and *O*-glycosylation events of serum CBG, which improve our understanding of molecular mechanisms governing the timely and tissue-specific delivery of cortisol to inflammatory sites. This work provides clues to molecular aberrations and disease mechanisms underpinning septic shock.

Keywords: CBG; cortisol; glycosylation; reactive centre loop; septic shock.

Introduction

Corticosteroid-binding globulin (CBG) is a serum glycoprotein produced primarily by hepatocytes and less by the gall bladder, kidney and other tissues (Hammond et al. 1987; Uhlén et al. 2015). CBG binds, transports and delivers cortisol and is therefore considered a principal regulator of this anti-inflammatory steroid hormone controlling its bioavailability to specific tissues (Siiteri et al. 1982; Westphal 1986; Perogamvros et al. 2012). In acute inflammation, hepatic synthesis of CBG is supressed leading to an increase in the free plasma cortisol level (Zouaghi et al. 1985; Bernier et al. 1998; Beishuizen et al. 2001; Ho et al. 2006; Dimopoulou et al. 2008). Recent clinical studies have highlighted the importance of CBG in septic shock, with CBG deficiency independently predicting patient mortality at ICU admission (Nenke et al. 2015; Meyer et al. 2019; Meyer et al. 2022; Lee et al. 2023).

CBG is a member of the serine protease inhibitor (serpin) superfamily and binds cortisol in a dedicated hydrophobic steroid-binding pocket. While CBG adopts the common three-dimensional structure of serpins including the characteristic reactive centre loop (RCL), it does not confer protease inhibition (Klieber et al. 2007; Gardill et al. 2012). Cortisol is eluted from CBG upon proteolytic cleavage of the RCL by neutrophil elastase (NE) found at sites of inflammation (Pemberton et al. 1988; Lee et al. 2025). Although the physiological relevance is still debated, other proteases including chymotrypsin and some exogenous virulence factors have also been found to cleave the RCL of CBG (Lewis and Elder 2014; Simard et al. 2014). At the inflammatory site, NE rapidly cleaves the RCL at Val344-Thr345 leading to profound stressed-to-relaxed conformational changes of CBG involving irreversible destruction of the cortisol-binding site, reduced cortisol binding affinity and, consequently, cortisol liberation from CBG (Fig. 1A) (Pemberton et al. 1988; Hammond et al. 1990). Temperature and pH are other factors reported to affect the CBG:cortisol binding affinity (Cameron et al. 2010; Meyer et al. 2020).

Protein glycosylation is increasingly recognised to impact many, if not most, immunomodulatory processes studied to date (Reily et al. 2019; Sackstein 2022). Fuelled by the growing appreciation of the diverse roles that glycans play in our blood and immune system, the glycobiology of CBG has attracted considerable attention over the past decades. Pioneered by Hammond and colleagues, CBG glycosylation was early on found to contribute to its steroid binding affinity and capacity (Hammond et al. 1991; Avvakumov et al.

Received: June 3, 2024. **Revised:** February 6, 2025. **Accepted:** February 21, 2025

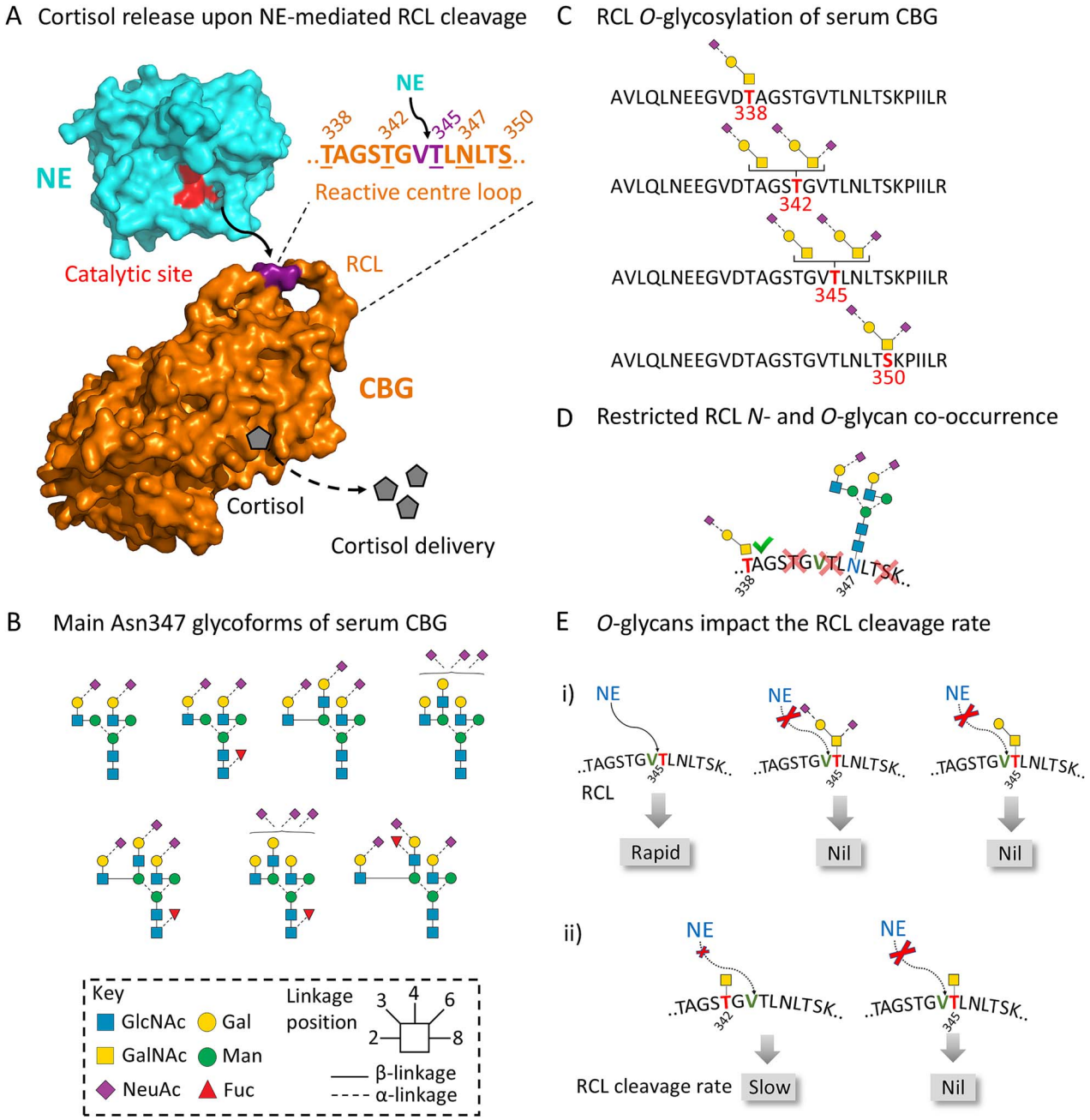

Fig. 1. Functional RCL *N*- and *O*-glycosylation events of CBG from healthy pooled sera. Overview of recently published findings (Chernykh et al. 2023). A. Release of cortisol upon neutrophil elastase (NE)-mediated cleavage of the reactive centre loop (RCL) of CBG as previously elucidated (Pemberton et al. 1988). Key amino acid residues of the RCL are shown. Panel B-E provide a summary of key RCL *N*- and *O*-glycosylation features of commercial CBG isolated from healthy pooled sera reported in our recent study (Chernykh et al. 2023). B. Main Asn347-glycans elucidated with fine structural details, see insert for symbol nomenclature and linkage key. C. Several RCL *O*-glycosylation sites carrying sialyl T and disialyl T were identified on serum CBG. D. RCL *O*- and *N*-glycan co-occurrence was exclusively found at Thr338 and Asn347. E. Impact of the *O*-glycan structures and their position on the relative RCL cleavage rate as documented for (i) recombinant CBG and (ii) synthetic RCL peptides. Figure adopted and further modified from *journal of biological chemistry* 2024;300(1):105519 with permission from Elsevier.

1993; Chan et al. 2013; Simard et al. 2018). Inspired by this foundational work implicating glycosylation in CBG function, we previously mapped the glycan compositions across the six known *N*-glycosylation sites of human serum CBG, revealing that heterogenous populations of heavily sialylated and fucosylated complex-type *N*-glycans decorate this cortisol-carrier protein (Sumer-Bayraktar et al. 2011). In a follow-up study aiming to detail the structure/function relationship of the Asn347-glycosylation strategically positioned near the NE cleavage site (Val344-Thr345) on the RCL, we found that the Asn347-glycans impact the NE-mediated RCL cleavage reaction, in part, by conferring steric hindrance of the RCL cleavage site (Sumer-Bayraktar et al. 2016).

Despite providing new mechanistic insight into the role of CBG glycans in cortisol delivery, these previous studies left some unaddressed questions regarding the important relationship between RCL glycosylation, proteolysis and cortisol release. For example, the fine structural details of the

Asn347-glycans were still missing representing a critical piece of information required to elucidate the RCL glycobiology. Furthermore, a recent large-scale *O*-glycoproteomics study of human sera provided clues to the presence of *O*-glycosylation at Thr342 on the RCL of CBG amongst several thousand other serum glycopeptides not validated or investigated further in that study (Yang et al. 2018). Collectively, this formed the rationale for setting out to perform a deep glycoprofiling and structure–function analysis of the RCL region of serum CBG.

Herein, we firstly summarise and reflect on our recently published LC–MS/MS-based discovery of coordinated RCL *N*- and *O*-glycosylation events on CBG from healthy donor sera (Chernykh et al. 2023), data discussed at the 2023 SfG Conference, Big Island, Hawaii. These findings are of significance as RCL *O*-glycans at Thr342 and Thr345 were found to inhibit the NE-mediated cleavage process implicating their involvement in cortisol delivery. We then investigate the clinical relevance of this discovery by using a similar LC–MS/MS-based approach to map the RCL *O*-glycosylation of serum CBG isolated from patients experiencing both less severe (moderate) and severe septic shock. We detail the structures and position of RCL *O*-glycans of serum CBG from septic shock individuals providing evidence to suggest a previously unknown link between RCL *O*-glycosylation and septic shock severity.

Results and discussion

Novel RCL O-glycans of CBG "cross-talk" with nearby N-glycans and inhibit RCL cleavage

In our recently published report (Chernykh et al. 2023), we used a multipronged LC–MS/MS-based characterisation strategy to comprehensively profile the RCL glycosylation of commercially available CBG isolated from pooled sera of healthy donors. These detailed biochemical analyses provided a quantitative view of the Asn347-glycans elucidated with fine structure details including their antennary branching patterns, sialyl linkage types and fucose placements (Fig. 1B), and revealed a previously unknown presence of *O*-glycosylation within the RCL region. The RCL *O*-glycans, which included both sialyl T and disialyl T (core 1-type) structures ($NeuAc_{1\text{-}2}Gal_1GalNAc_1$), were observed across multiple sites (Thr338, Thr342, Thr345, Ser350) in vicinity of both the Asn347 glycosylation site and the cleavage site targeted by NE (Val344-Thr345) (Fig. 1C).

Interestingly, in this commercial form of serum CBG, only one of the *O*-glycosylation sites (Thr338) demonstrated an *O*-glycan co-occurrence with an Asn347-linked *N*-glycan on the same RCL molecule (Fig. 1D). The interplay ("crosstalk") between adjacent *N*- and *O*-glycosylation events, which we supported by in silico modelling, is an interesting phenomenon also reported by several other groups for different proteins (Stavenhagen et al. 2018; Bagdonaite et al. 2021; Tian et al. 2021; Chien et al. 2023; Wei et al. 2023; Chongsaritsinsuk et al. 2024).

We then investigated GalNAc-T isoenzymes responsible for the observed RCL *O*-glycosylation events. We focused on GalNAc-T2 and GalNAc-T3 as these mucin-type *O*-glycosylation initiating enzymes are abundantly expressed in liver and gall bladder, respectively, the two main tissue origins of serum CBG (Bennett et al. 2012; Uhlén et al. 2015). Both GalNAc-T2 and GalNAc-T3 isoenzymes demonstrated an ability to effectively transfer GalNAc residues to multiple sites of a synthetic RCL peptide. While these in vitro observations putatively link GalNAc-T2 and GalNAc-T3 to the RCL *O*-glycosylation process, future in vivo studies are required to confirm this relationship and identify the tissue origin(s) of the *O*-glycosylated CBG glycoforms found in serum.

We then investigated the functional role of the newly discovered RCL *O*-glycosylation and focused on exploring how *O*-glycans at Thr345 located directly at the NE cleavage site (Val344-Thr345) may impact the NE-mediated RCL proteolysis reaction. LC–MS/MS was used to longitudinally monitor the proteolysis reaction of both a native and an asialovariant of HEK293-derived recombinant CBG, which conveniently was found to carry almost exclusively Thr345 *O*-glycosylation on the RCL. Both sialylated (disialyl T) and asialylated (T) core 1-type *O*-glycans at the Thr345 site strongly inhibited the NE-mediated proteolysis reaction compared to the prompt cleavage of non-glycosylated RCL (Fig. 1E, i). These experimental findings were supported by MD simulations of NE in complex with glycosylated RCL showing in silico that both elongated and truncated *O*-glycans at Thr345 strongly interfere with NE by impairing its accessibility to the RCL cleavage site. Finally, we also used MALDI-MS profiling to longitudinally survey the NE-mediated RCL proteolysis reaction of a set of defined RCL peptides synthetised with and without a GalNAc residue at Thr342 or Thr345. While the non-glycosylated RCL peptide was promptly cleaved, the RCL peptide carrying *O*-glycosylation at Thr342 and Thr345 conferred moderate and strong protection against NE proteolysis, respectively (Fig. 1E, ii).

Collectively, in our recently published study (Chernykh et al. 2023) we reported on novel and coordinated RCL *N*- and *O*-glycosylation events of CBG from pooled sera of healthy donors and demonstrated that RCL *O*-glycans at Thr342 and Thr345 inhibit the NE-mediated RCL proteolysis process important for cortisol delivery.

RCL O-glycosylation levels in septic shock sera associate with disease severity

To investigate the clinical relevance of the newly discovered RCL *O*-glycosylation of serum CBG, we decided to focus on septic shock since CBG and cortisol depletion are recognised features of this disease (Meyer et al. 2022; Fowler et al. 2023). Sepsis is characterised as life-threatening organ dysfunction caused by an unbalanced and often exaggerated immune response to pathogenic insult, while septic shock is defined as a subset of sepsis with profound cellular, circulatory and metabolic abnormalities (Singer et al. 2016). Despite progress in understanding the complex molecular and cellular mechanisms underpinning these systemic conditions (Zhang and Ning 2021), no significant advances have been achieved in the treatment of septic shock patients over the past decades and mortality and morbidity remain unacceptably high (Rudd et al. 2020).

To explore the potential link between CBG RCL *O*-glycosylation and septic shock, we immuno-affinity purified CBG from blood sera collected at the time of ICU admission of twelve septic shock patients presenting with moderate ($n = 6$) and severe ($n = 6$) illness (see Table 1 for key patient data). We then used similar sample preparation and LC–MS/MS approaches as applied to CBG from healthy serum (Chernykh et al. 2023) to profile the RCL *O*-glycosylation of CBG from septic shock serum. To ease the identification and enable a

Table 1. Baseline characteristics and outcomes of the cohort of septic shock patients.

	Moderate septic shock (n = 6)	Severe septic shock (n = 6)
Patient characteristics		
Age, years	64.8 ± 11.9	51.7 ± 23.5
Sex (males)	0/6 (0%)	2/6 (33%)
BMI	26.5 ± 5.6	30.3 ± 4.8
Diabetes	0/6 (0%)	1/6 (16.7%)
Immunocompromised	1/6 (16.7%)	0/6 (0%)
APACHE II score[a]	17.7 ± 4.5	18.0 ± 4.6
SOFA score[b]	8.0 ± 2.6	11.2 ± 2.0
Hydrocortisone use	0/6 (0%)	0/6 (0%)
Physiological values[c]		
CBG, nmol/L	317.1 ± 111.8	283.6 ± 164.6
ACTH, pmol/L	3.2 ± 1.7	7.1 ± 11.5
Lactate, mmol/L	4.1 ± 1.8	3.6 ± 3.0
White cell count, 10^9/cells/L	24.7 ± 12.2	12.7 ± 6.1
Outcomes		
ICU mortality	0/6 (0%)	0/6 (0%)
28-day mortality	0/6 (0%)	0/6 (0%)
90-day mortality	0/6 (0%)	1/6 (16.7%)
Mechanical ventilation	4/6 (66.7%)	6/6 (100%)
Renal replacement therapy	0/6 (0%)	0/6 (0%)
Norepinephrine (noradrenaline)		
Total dose (μg)	15,785.8 ± 8,622.7	52,391.5 ± 36,529.5
Duration (days)	1.4 ± 0.5	3.2 ± 1.8
Physiological correlates[c]		
IL-6 (pg/mL)	776.6 ± 808.4	923.1 ± 1,619.34
TNFα (pg/mL)	89.7 ± 59.7	80.9 ± 27.2
α1AT (g/L)	2.3 ± 0.4	2.1 ± 0.5

Data are given as mean ± SD and n or n/total n (%). Abbreviations: α1AT, α-1-antitrypsin; ACTH, adrenocorticotropic hormone; APACHE II, acute physiology and chronic health evaluation II; BMI, body mass index; CBG, corticosteroid-binding globulin; ICU, intensive care unit; IL-6, interleukin-6; TNFα, tumour necrosis factor α. [a]Scores on the APACHE II are assessed on a scale from 0 to 71, with higher scores indicating a higher risk of death. [b]Scores on the SOFA range from 0 to 24, with higher scores indicating greater severity of illness. The baseline SOFA score was calculated from admission data. [c]The values represent the most recent results when admitted with septic shock.

quantitative analysis, any interfering Asn347-glycans were enzymatically removed from the RCL peptides prior to the *O*-glycan profiling. RCL *O*-glycosylation decorating exclusively the Thr342 site in the form of sialyl T and/or disialyl T structures was consistently detected of serum CBG from all septic shock patients (Fig. 2A, see Supplementary Fig. S1-S17 for spectral evidence). These two *O*-glycoforms were found on RCL peptides with and without Asn347 deamidation, indicating that the Thr342 *O*-glycans, at least in part, may co-exist with an Asn347-glycan on CBG from septic shock sera. These new experimental findings are interesting as they suggest that, in septic shock, RCL *N*- and *O*-glycan co-occupancy is not restricted to *O*-glycans positioned at Thr338 (Fig. 1D). Future in silico modelling of GalNAc-T isoenzymatic variants other than GalNAc-T2 (e.g. GalNAc-T3) supported by experimental observations are warranted to explore further the molecular basis of the cross-talk of the RCL *N*- and *O*-glycans of serum CBG in septic shock.

Contrasting the intermediate levels of disialyl T (∼40%) found on the RCL from CBG of healthy pooled sera (Chernykh et al. 2023), the septic shock patients exhibited a higher level of disialyl T (60–100%) (Fig. 2B). No apparent differences in the *O*-glycoform distribution were identified between patients with moderate and severe illness. The elevated disialyl T levels in septic shock serum are potentially interesting as both glycan branching and sialylation add considerable volume to the RCL *O*-glycan moiety and therefore are likely to affect its ability to sterically hinder the NE-mediated RCL proteolytic process. We have previously established that a single GalNAc residue at Thr342 moderately inhibits the NE cleavage reaction (Fig. 1E, ii) (Chernykh et al. 2023). The observation that elongated and branched RCL *O*-glycans decorate Thr342 of serum CBG in septic shock suggests their ability to inhibit NE-mediated RCL proteolysis and potentially impact cortisol delivery in septic shock, speculations awaiting further exploration.

Four utilised *O*-glycosylation sites were identified within the RCL region of CBG from pooled sera of healthy donors (Thr338, Thr342, Thr345 and Ser350) (Chernykh et al. 2023), but we were in that study unable to reliably determine which site(s) were the most prevalent due to co-elution of the *O*-glycopeptide site isomers. In contrast, we found only one utilised *O*-glycosylation site (Thr342) when investigating CBG from septic shock sera. Reinterrogation of a publicly available *O*-glycoproteomics (site-focused) dataset of healthy human serum (Yang et al. 2018) indicated that Thr342 *O*-glycosylation (15 glycoPSMs identified) is more prevalent than Thr345 (2 glycoPSMs identified, data not shown). This points to Thr342 being the dominant *O*-glycosylation site of CBG from healthy human serum and thereby provides a plausible explanation as to why only the Thr342 site was identified from the limited amount of CBG available from septic shock serum analysed in this study.

Interestingly, the total RCL *O*-glycosylation level was found to correlate with the severity of the septic shock illness. Relative to the RCL *O*-glycosylation levels of less severe (moderate) cases (1.79% ± 0.70%), individuals with severe illness displayed elevated RCL *O*-glycosylation (3.03% ± 1.49%, $P < 0.05$) (Fig. 2C). While relatively high inter-patient variations were observed (likely due to septic shock being a

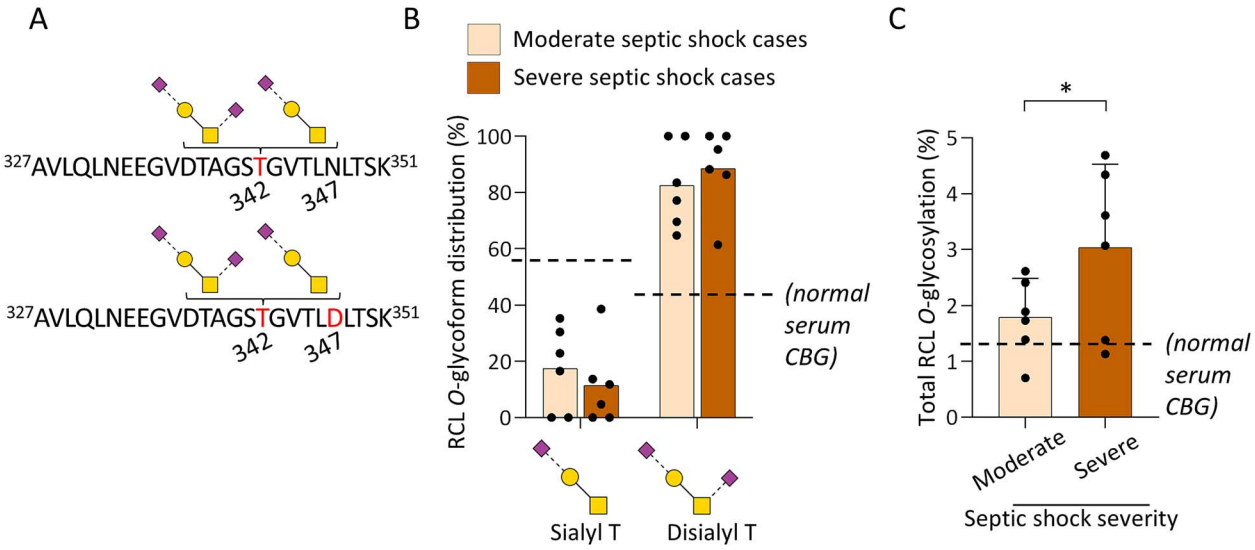

Fig. 2. RCL *O*-glycosylation of CBG isolated from septic shock sera. A. Overview of RCL *O*-glycoforms decorating Thr342 of CBG isolated from serum of twelve septic shock patients, see supplementary Fig. S1–S5 for annotated EThcD-MS/MS spectra evidencing the site localisation and supplementary Fig. S6–S17 for annotated HCD-MS/MS data detailing the site-specific *O*-glycoprofile. RCL *O*-glycosylation was observed both with and without Asn347 deamidation indicating partial co-existence with an RCL *N*-glycan. B. RCL *O*-glycoform distribution of serum CBG from septic shock patients presenting with moderate (n = 6) and severe (n = 6) illness upon ICU admission. C. Total RCL *O*-glycosylation level of serum CBG from the septic shock patient cohort. Bars are plotted as mean ± SD, n = 6 for each group, student t-test. $^*P < 0.05$. For B and C, dashed lines indicate the average level established for CBG from pooled sera of healthy donors (Chernykh et al. 2023).

highly heterogeneous disease), the RCL *O*-glycosylation levels of CBG from septic shock sera were generally higher than levels observed from CBG isolated from healthy donor sera (1.25% ± 0.13%) (Chernykh et al. 2023). The higher RCL *O*-glycosylation levels in patients experiencing severe septic shock is interesting as it, given the likely inhibitory effects of the elongated and branched Thr342 *O*-glycans (disialyl T, see above), points to reduced RCL cleavage and cortisol release rates in the most critically sick individuals. However, given the large variations in RCL *O*-glycosylation amongst patients experiencing severe septic shock and confounded by the difficulties of accurately stratifying patients according to their septic shock disease severity, these interesting trends warrant further exploration in larger patient cohorts. In addition to the relatively small cohort size (n = 6 patients per group), gender imbalance within the two patient groups was another limitation of our study. Patients with moderate illness were all females, whereas patients with severe illness comprised both females (66%) and males (33%). While the small cohort size and an imperfect gender match between the patient groups reflect the considerable challenges in recruiting and accurately stratifying patients, these limitations may be important as protein glycosylation is known to be impacted by gender (Dotz and Wuhrer 2019; Gizaw et al. 2019; Lado-Baleato et al. 2023). However, exploring our glycopeptide data for any gender bias, we note that the total RCL *O*-glycosylation level was still significantly different between the moderate and severe septic shock group when excluding the two males from the latter patient group (now n = 4, data not shown). Together with the fact that the RCL *O*-glycosylation level of the two male patients were well within the distribution of data points from the female patients, this indicates that gender may not impact the conclusions of this CBG-focused study. Regardless, a follow up study using larger and gender- and age-matched cohorts of septic shock patients are warranted to validate the findings reported herein.

Several studies have reported on aberrant glycosylation in sepsis. For example, septic patients were found to display glycosylation changes in α-1-antichymotrypsin, IgG, transferrin and neat serum upon ICU admission or over the disease course (Piagnerelli et al. 2005; Gornik et al. 2007; Gornik et al. 2011; de Haan et al. 2018; Caval et al. 2020). Some studies also reported on glycosylation features that showed a potential to stratify septic shock severity and predict disease outcome (Brinkman-Van Der Linden et al. 1996; Gornik et al. 2011; DeCoux et al. 2015; de Haan et al. 2018). Most studies, however, explored *N*-glycosylation changes in sepsis and we found only few reports about *O*-glycosylation. Lin and colleagues studied the effect of gene polymorphism and acute inflammation on the *N*- and *O*-glycosylation of serum fetuin in healthy donors and septic shock patients and stratified these individuals based on their proteoform profiles (Lin et al. 2019). Another study found a correlation between the ratios of *O*-glycosylated proteoforms of apolipoprotein C-III and mortality in severe sepsis (Harvey et al. 2009). Additionally, one study showed that core 1- and core 3-type *O*-glycans are increased in bacterial septic mice relative to uninfected controls (Heindel et al. 2022). Our study adds to these examples suggesting that protein- and position-specific *O*-glycosylation changes occur in septic shock patients presenting with the most critical conditions.

In summary, this work has detailed structure–function relationships of complex RCL-specific *N*- and *O*-glycosylation patterns of serum CBG in the context of RCL cleavage, cortisol release and septic shock. In our recently published study (Chernykh et al. 2023), we discovered previously unknown RCL *O*-glycosylation events, and elucidated their position-specific interplay with RCL *N*-glycans and their inhibitory role in NE-mediated proteolysis of the RCL critical for cortisol delivery. Prompted by these findings, we explored the RCL *O*-glycosylation of serum CBG in a cohort of septic shock patients, which pointed to an interesting relationship

between Thr342 RCL *O*-glycosylation and disease severity. Our work contributes to an improved understanding of mechanisms governing CBG-guided cortisol delivery to sites of inflammation and highlights the complex nature and functional importance of CBG glycosylation in that process. Taken together with our previous clinical study linking septic shock mortality with CBG deficiency (Meyer et al. 2022), and the recommended use of low dose corticosteroids in septic shock patients who are not responsive to fluid and moderate-to-high dose vasopressor therapy (Annane et al. 2017; Evans et al. 2021), our study has established fundamental knowledge that may eventually open avenues for clinical trials investigating CBG supplementation in septic shock.

Materials and methods

This method section pertains to the new experiments and data analyses communicated in this paper. For methods and materials related to previously published experiments and results, please refer to our communicated research paper (Chernykh et al. 2023).

Key materials

Elizabethkingia miricola peptide:*N*-glycosidase F (PNGase F) recombinantly expressed in *E. coli* was from Promega (catalogue number 9PIV483). Modified porcine trypsin was from Promega (catalogue number V5111). Ultra-high-quality water was used for all experiments. All chemicals and LC solvents were from Sigma Aldrich/Thermo Fisher Scientific unless otherwise specified.

Septic shock patients

Whole blood (~10 mL/drawing) was collected from twelve septic shock patients receiving norepinephrine infusion upon admission to ICU at the Royal Adelaide Hospital, Adelaide, Australia. Blood serum from circulating morning blood samples was stored at −80 °C until analysis. Data were collected and recorded in the web-based Research Electronic Data Capture (REDCap) software (v11.0.3, Nashville, TN, USA). All aspects of patient care were conducted at the discretion of the treating clinician. Septic shock was clinically diagnosed according to the Sequential Organ Failure Assessment (SOFA). Participants were defined has having moderate or severe septic shock based on noradrenaline requirements (duration for less than or greater than 48 h, and total dose, respectively), SOFA and Acute Physiology and Chronic Health Evaluation II (APACHE II) scores. Six individuals presented with moderate illness (n = 6) while another six individuals presented with severe illness (n = 6), see Table 1 for key patient data. Informed consents were obtained for all participants and the work was approved by The Central Adelaide Local Health Network Human Research Ethics Committee (Protocol no. R20160208 HREC/16/RAH/29) as part of a larger study of CBG in septic shock (Meyer et al. 2022). As the study did not involve therapeutic intervention, the research did not require registration with the Australian New Zealand Clinical Trials Registry.

Immuno-affinity purification of serum CBG

12G2 mAbs from 12G2 hybridomas were generously donated by Dr John Lewis, Christchurch, New Zealand. Hybridomas were expanded in RPMI 1640 growth media (Gibco) supplemented with glutamine, penicillin/streptomycin, adenine, aminopterin, thymidine and 10% (w/w) foetal calf serum. The hybridoma underwent direct adaptation to PFHM-II protein-free hybridoma media (Thermo Fisher Scientific) supplemented with penicillin/streptomycin and glutamine. The supernatant was collected after centrifugation, filtered through a 0.2 μm filter, and applied to a protein G chromatography cartridge (Pierce) at 1.6 mL/min using a peristaltic pump. The 12G2 mAbs were eluted from the cartridge using 0.1 M glycine, pH 2.55, neutralised with 1 M Tris, and dialysed against PBS using a 10 kDa MWCO dialysis cassette (Thermo Fisher Scientific). Purified antibodies were concentrated using Vivaspin2 (Sartorius) to achieve a 12G2 mAb concentration of ~1 mg/mL and were coupled to tosyl-activated Dynabeads (Thermo Fisher Scientific) over 24 h at 38 °C in 0.1 M borate buffer, pH 9.5, with 1 M ammonium sulphate. For serum CBG isolation, 1 mg 12G2 mAb coupled to Dynabeads was incubated with 125 μL patient serum for 1 h, washed with PBS with 0.5% (v/v) Tween20, followed by plain PBS washes. CBG was eluted from the Dynabeads using 0.1 M glycine, pH 2.55, and subsequently neutralised with 500 mM ammonium bicarbonate, and dried.

Sample preparation of CBG

The dried CBG protein pellets were dissolved in 23 μL lysis buffer containing 5% (w/v) SDS in 50 mM triethylammonium bicarbonate buffer (TEAB), pH 8.5. Reduction and alkylation were performed using 5 mM dithiothreitol for 45 min at 56 °C and 20 mM iodoacetamide (final concentrations) for 30 min in dark, respectively. Subsequently, 2.5% (v/v) phosphoric acid (final concentration) was added to denature CBG and samples were vortexed. This was followed by adding a 6-fold volume of binding/wash buffer containing 100 mM TEAB in 90% (v/v) methanol, pH 7.55. Samples were transferred to S-Trap mini columns (Protifi, Fairport, NY) and centrifuged at 4,000 g for 30 s. The immobilised CBG was washed three times with binding/wash buffer and centrifuged at 4,000 g for 1 min to remove the binding/wash buffer. Subsequently, 20 μL digestion buffer containing 1 μg trypsin/sample (sequencing grade, Promega) in 50 mM TEAB was added to the S-trap columns. Trypsin digestion was performed overnight at 37 °C. The resultant peptide mixtures were sequentially eluted with 40 μL 50 mM TEAB in water, 40 μL 0.2% (v/v) formic acid (FA) in water and 40 μL 50% (v/v) acetonitrile (ACN) in water. Eluted fractions were collected after centrifugation, combined and dried. CBG peptides were de-*N*-glycosylated using 10 U PNGase F (Promega) in 20 μL 50 mM ammonium bicarbonate (16 h, 37 °C), dried and kept at −30 °C until use. Peptides were resuspended in 0.1% (v/v) FA prior to LC–MS/MS.

LC–MS/MS

To enable comparisons to the glycoprofile of CBG from healthy pooled serum (Chernykh et al. 2023), LC–MS/MS experiments using similar acquisition conditions were performed to i) localise the RCL *O*-glycosylation site(s) and ii) determine the RCL *O*-glycoform distribution on CBG isolated from septic shock sera.

i) Peptides were analysed on an Orbitrap Eclipse Tribrid Mass Spectrometer coupled to a Vanquish Neo UHPLC system (Thermo Fisher Scientific). Peptides were separated on a reversed-phase Double nanoViper™ PepMap™ Neo C18 LC

column (75 μm inner diameter × 150 mm column length, 2 μm particle size, Thermo Fisher Scientific). For this, a gradient of 2.5%–40% (v/v) solvent B (80% ACN containing 0.1% [both v/v] aqueous FA) over 52 min in solvent A consisting of 0.1% (v/v) aqueous FA was employed at 300 nL/min, 45 °C. The mass spectrometer was operated in positive ion polarity mode. Full MS1 scans were acquired with a scan range of *m/z* 350–2,000 at a resolution of 120,000 full width at half maximum (FWHM, measured at *m/z* 200), standard AGC target, and 50 ms maximum injection time. DDA was used to generate MS/MS data following precursor ion selection and isolation using a quadrupole isolation window of *m/z* 2.0. Higher-energy collisional dissociation (HCD)–MS/MS was performed at top speed with 30% normalised collision energy (NCE) with fragment ions detected in the Orbitrap using 30,000 resolution, standard AGC target, and 60 ms maximum injection time. Re-isolation and electron transfer higher-energy collision dissociation (EThcD)-MS/MS fragmentation of select precursor ions were triggered by the presence of at least one of three specific diagnostic oxonium ions i.e. *m/z* 204.0867 (HexNAc), *m/z* 138.0545 (HexNAc fragment), and *m/z* 366.1396 (HexHexNAc) among the twenty most intense fragment ions in each HCD–MS/MS spectrum (15 ppm mass tolerance). EThcD–MS/MS of precursors isolated with a quadrupole isolation window of *m/z* 2.0 was performed with a supplemental activation energy of NCE 25%. Fragment ions were detected in the Orbitrap using 30,000 resolution, 200% AGC target and 200 ms maximum injection time. All MS and MS/MS data were acquired in profile mode.

ii) Peptides were loaded on a trap column (0.1 mm inner diameter x 20 mm column length) custom-packed with ReproSil-Pur C18-AQ 5 μm resin (Dr. Maisch, Germany) operated by an UltiMate 3000 RSLCnano HPLC system (Thermo Fisher Scientific). Approximately 300 ng CBG peptide material was injected and separated at a constant flow rate of 300 nL/min at 45 °C on a custom-made Reprosil-Pur 120 C18-AQ analytical LC column (3 μm particle size, 300 mm column length × 0.075 mm inner diameter, Dr. Maisch GmbH, Germany). The mobile phases were 0.1% FA in 99.9% (both v/v) ACN (solvent B) and 0.1% (v/v) aqueous FA (solvent A). The gradient of solvent B increased from 2%–15% (v/v) over 5 min, 15%–33% (v/v) over 25 min, 33%–95% (v/v) over 5 min, and, finally, 6 min at 95% B (v/v). The nano-LC was connected to a Q-Exactive HF-X Hybrid Quadrupole-Orbitrap mass spectrometer (Thermo Fisher Scientific) operating in positive ion polarity mode. Full MS1 scans were acquired in the Orbitrap with an AGC target of 3×10^6 ions and a maximum fill time of 60 ms. MS1 scans were acquired at a resolution of 120,000 FWHM (at *m/z* 200) with a range of *m/z* 450–2,000. Data-dependant acquisition was used to collect MS/MS data of the 20 most abundant precursor ions in each MS1 full scan utilising HCD with NCE of 28%. Precursors selected for fragmentation were at least doubly charged. Fragment ions were measured at a resolution of 15,000 FWHM (at *m/z* 200) with an AGC target of 2×10^5 ions and a maximum injection time of 28 ms using a precursor isolation window of *m/z* 1.2.

Data analysis

All LC–MS/MS raw data were browsed using Xcalibur v2.2 (Thermo Fisher Scientific). The HCD- and EThcD-MS/MS data were searched against the canonical sequence of human CBG (UniProtKB, P08185). Decoy and contaminant databases were enabled to establish the false discovery rate (FDR) of peptide candidates. The precursor and product ion mass tolerance were 10 and 20 ppm, respectively. Peptides with a semi-specific trypsin cleavage pattern (C-terminal to R/K) were considered with a maximum of one missed tryptic cleavage site per peptide. Searches were performed with carbamidomethylation of Cys (+57.021 Da) as a fixed modification. Oxidation of Met (+15.994 Da) and deamidation of Asn (+0.9840 Da) were considered as common variable modifications. *N*-glycosylation of sequon-localised Asn and *O*-glycosylation of any Thr/Ser residue were considered as rare modifications and candidates were identified from predefined glycan databases (182 human *N*-glycans and 70 human *O*-glycans). *N*-glycans were included in the search as a control to ensure complete de-*N*-glycosylation with PNGase F. One or two rare and a total of two common modifications were permitted per peptide. All searches were filtered to <1% FDR at the protein level and 0% at the peptide level. A PEP-2D score < 0.001 was used as a general confidence threshold to filter glycopeptide candidates. The Byonic-identified *O*-glycopeptide candidates were manually scrutinised to ensure correct annotation.

The relative abundance of the observed RCL (glyco)peptides was quantified using area-under-the-curve (AUC) measurements based on extracted ion chromatograms (XICs) generated from the monoisotopic precursor ions of all identified (glyco)peptide species in all detected charge states using Skyline v21.1 (Schilling et al. 2012). The RCL *O*-glycoform distribution was established by calculating the proportion of the AUC of the individual *O*-glycopeptide forms relative to the total AUC of all RCL *O*-glycopeptide forms, an approach commonly employed in quantitative glycopeptide analysis (Rebecchi et al. 2009; Thaysen-Andersen et al. 2015; Tjondro et al. 2020). The total RCL *O*-glycosylation level was determined as the proportion of the combined AUC of all *O*-glycosylated RCL peptides relative to the total AUC of all observed RCL peptides. For the quantitation of the RCL *O*-glycoform distribution and to determine the overall *O*-glycosylation levels both the de-*N*-glycosylated (formerly Asn347-glycosylated) and non-*N*-glycosylated RCL peptide forms were considered.

Data visualisation and statistics

For each patient group, bars have been plotted as the mean, while their error bars represent standard deviation (SD). The individual data points have also been shown for the bar graphs. Data were visualised using GraphPad Prism v9.5.1 (Dotmatics). Comparative statistical analyses were performed using a one-tailed student's t-test with the confidence threshold of $P < 0.05$. A hypothesis-driven statistical approach was justified as preliminary data (n = 1/patient group) indicated that the RCL *O*-glycosylation level is elevated in septic shock patients with severe illness relative to less severe cases (data not shown).

Acknowledgments

The study was supported by AusHealth, Adelaide, SA, Australia. AC was supported by a Research Training Program scholarship funded by the Australian Government. JHL was supported by Dawes Scholarship from the Royal Adelaide Hospital Research Fund and Margorie Hooper Travel Grant from the RACP Foundation. EJM is supported by

the Royal Adelaide Hospital Research Committee 2023 Early Career Research Fellowship (MYIP 17236]. MTA is the recipient of an ARC Future Fellowship (FT210100455).

Author contributions

Anastasia Chernykh (Conceptualization [supporting], Data curation [lead], Formal analysis [lead], Investigation [lead], Methodology [lead], Visualization [lead]), Zeynep Sumer-Bayraktar (Conceptualization [supporting], Data curation [supporting], Formal analysis [supporting], Investigation [supporting], Methodology [supporting], Software [supporting], Visualization [supporting]), Jessica H Lee (Data curation [supporting], Formal analysis [supporting], Investigation [supporting], Methodology [supporting]), Emily J Meyer (Data curation [supporting], Formal analysis [supporting], Funding acquisition [equal], Investigation [supporting], Methodology [supporting], Project administration [supporting], Resources [supporting], Software [supporting], Supervision [supporting], Visualization [supporting]), David J Torpy (Conceptualization [supporting], Funding acquisition [equal], Investigation [supporting], Project administration [supporting], Resources [supporting], Supervision [supporting]), Morten Thaysen-Andersen (Conceptualization [lead], Data curation [supporting], Formal analysis [supporting], Funding acquisition [equal], Investigation [supporting], Methodology [supporting], Project administration [lead], Resources [lead], Software [supporting], Supervision [lead]).

Supplementary material

Supplementary material is available at *Glycobiology Journal* online.

Funding

None declared.

Conflict of interest statement

None declared.

Data availability

All LC–MS/MS raw data generated for this study have been made available through ProteomeXchange Consortium *via* the PRIDE repository (PXD058963) (Perez-Riverol et al. 2022).

References

Annane D et al. 2017. Guidelines for the diagnosis and management of critical illness-related corticosteroid insufficiency (CIRCI) in critically ill patients (part I): Society of Critical Care Medicine (SCCM) and European Society of Intensive Care Medicine (ESICM) 2017. *Intensive Care Med*. **43**:1751–1763. https://doi.org/10.1007/s00134-017-4919-5.

Avvakumov GV, Warmels-Rodenhiser S, Hammond GL. 1993. Glycosylation of human corticosteroid-binding globulin at aspargine 238 is necessary for steroid binding. *J Biol Chem*. **268**:862–866. https://doi.org/10.1016/S0021-9258(18)54013-8.

Bagdonaite I et al. 2021. Site-specific O-glycosylation analysis of SARS-CoV-2 spike protein produced in insect and human cells. *Viruses*. **13**:551. https://doi.org/10.3390/v13040551.

Beishuizen A, Thijs LG, Vermes I. 2001. Patterns of corticosteroid-binding globulin and the free cortisol index during septic shock and multitrauma. *Intensive Care Med*. **27**:1584–1591. https://doi.org/10.1007/s001340101073.

Bennett EP et al. 2012. Control of mucin-type O-glycosylation: a classification of the polypeptide GalNAc-transferase gene family. *Glycobiology*. **22**:736–756. https://doi.org/10.1093/glycob/cwr182.

Bernier J, Jobin N, Emptoz-Bonneton A, Pugeat MM, Garrel DR. 1998. Decreased corticosteroid-binding globulin in burn patients: relationship with interleukin-6 and fat in nutritional support. *Crit Care Med*. **26**:452–460. https://doi.org/10.1097/00003246-199803000-00014.

Brinkman-Van Der Linden EC, Van Ommen EC, Van Dijk W. 1996. Glycosylation of alpha 1-acid glycoprotein in septic shock: changes in degree of branching and in expression of sialyl Lewis^x groups. *Glycoconj J*. **13**:27–31. https://doi.org/10.1007/BF01049676.

Cameron A et al. 2010. Temperature-responsive release of cortisol from its binding globulin: a protein thermocouple. *J Clin Endocrinol Metab*. **95**:4689–4695. https://doi.org/10.1210/jc.2010-0942.

Caval T et al. 2020. Glycoproteoform profiles of individual Patients' plasma Alpha-1-Antichymotrypsin are unique and extensively Remodeled following a septic episode. *Front Immunol*. **11**:608466. https://doi.org/10.3389/fimmu.2020.608466.

Chan WL, Carrell RW, Zhou A, Read RJ. 2013. How changes in affinity of corticosteroid-binding globulin modulate free cortisol concentration. *J Clin Endocrinol Metab*. **98**:3315–3322. https://doi.org/10.1210/jc.2012-4280.

Chernykh A et al. 2023. Position-specific N- and O-glycosylation of the reactive center loop impacts neutrophil elastase-mediated proteolysis of corticosteroid-binding globulin. *J Biol Chem*. **300**:105519. https://doi.org/10.1016/j.jbc.2023.105519.

Chien YC et al. 2023. High density of N- and O-glycosylation shields and defines the structural dynamics of the intrinsically disordered Ectodomain of receptor-type protein tyrosine phosphatase alpha. *JACS Au*. **3**:1864–1875. https://doi.org/10.1021/jacsau.3c00124.

Chongsaritsinsuk J et al. 2024. Quantification and site-specific analysis of Co-occupied N- and O-Glycopeptides. *J Proteome Res*. **23**:5449–5461. https://doi.org/10.1021/acs.jproteome.4c00574.

DeCoux A et al. 2015. Plasma Glycoproteomics reveals sepsis outcomes linked to distinct proteins in common pathways. *Crit Care Med*. **43**:2049–2058. https://doi.org/10.1097/CCM.0000000000001134.

Dimopoulou I et al. 2008. Pituitary-adrenal responses following major abdominal surgery. *Hormones (Athens)*. **7**:237–242. https://doi.org/10.14310/horm.2002.1203.

Dotz V, Wuhrer M. 2019. N-glycome signatures in human plasma: associations with physiology and major diseases. *FEBS Lett*. **593**:2966–2976. https://doi.org/10.1002/1873-3468.13598.

Evans L et al. 2021. Surviving sepsis campaign: international guidelines for management of sepsis and septic shock 2021. *Intensive Care Med*. **47**:1181–1247. https://doi.org/10.1007/s00134-021-06506-y.

Fowler C, Raoof N, Pastores SM. 2023. Sepsis and adrenal insufficiency. *J Intensive Care Med*. **38**:987–996. https://doi.org/10.1177/08850666231183396.

Gardill BR, Vogl MR, Lin HY, Hammond GL, Muller YA. 2012. Corticosteroid-binding globulin: structure-function implications from species differences. *PLoS One*. **7**:e52759. https://doi.org/10.1371/journal.pone.0052759.

Gizaw ST, Gaunitz S, Novotny MV. 2019. Highly sensitive O-glycan profiling for human serum proteins reveals gender-dependent changes in colorectal cancer patients. *Anal Chem*. **91**:6180–6189. https://doi.org/10.1021/acs.analchem.9b00822.

Gornik O et al. 2007. Changes of serum Glycans during sepsis and acute pancreatitis. *Glycobiology*. **17**:1321–1332. https://doi.org/10.1093/glycob/cwm106.

Gornik O, Gornik I, Kolednjak IZ, Lauc G. 2011. Change of transferrin sialylation differs between mild sepsis and severe sepsis and septic shock. *Intern Med*. **50**:861–869. https://doi.org/10.2169/internalmedicine.50.4704.

de Haan N et al. 2018. Differences in IgG Fc glycosylation are associated with outcome of Pediatric meningococcal *Sepsis mBio*. **9**:e00546–e00518. https://doi.org/10.1128/mBio.00546-18.

Hammond GL et al. 1987. Primary structure of human corticosteroid binding globulin, deduced from hepatic and pulmonary cDNAs, exhibits homology with serine protease inhibitors. *Proc Natl Acad Sci*. **84**:5153–5157. https://doi.org/10.1073/pnas.84.15.5153.

Hammond GL, Smith CL, Paterson NAM, Sibbald WJ. 1990. A role for corticosteroid-binding globulin in delivery of cortisol to

activated neutrophils. *J Clin Endocrinol Metab*. **71**:34–39. https://doi.org/10.1210/jcem-71-1-34.

Hammond GL, Smith CL, Underhill DA. 1991. Molecular studies of corticosteroid binding globulin structure, biosynthesis and function. *J Steroid Biochem Mol Biol*. **40**:755–762. https://doi.org/10.1016/0960-0760(91)90300-T.

Harvey SB et al. 2009. O-glycoside biomarker of apolipoprotein C3: responsiveness to obesity, bariatric surgery, and therapy with metformin, to chronic or severe liver disease and to mortality in severe sepsis and graft vs host disease. *J Proteome Res*. **8**:603–612. https://doi.org/10.1021/pr800751x.

Heindel DW et al. 2022. Glycomic analysis reveals a conserved response to bacterial sepsis induced by different bacterial pathogens. *ACS Infect Dis*. **8**:1075–1085. https://doi.org/10.1021/acsinfecdis.2c00082.

Ho JT et al. 2006. Septic shock and sepsis: a comparison of Total and free plasma cortisol levels. *J Clin Endocrinol Metab*. **91**:105–114. https://doi.org/10.1210/jc.2005-0265.

Klieber MA, Underhill C, Hammond GL, Muller YA. 2007. Corticosteroid-binding globulin, a structural basis for steroid transport and proteinase-triggered release. *J Biol Chem*. **282**:29594–29603. https://doi.org/10.1074/jbc.M705014200.

Lado-Baleato O et al. 2023. Age-related changes in serum N-Glycome in men and women-clusters associated with comorbidity. *Biomol*. **14**:17. https://doi.org/10.3390/biom14010017.

Lee JH, Meyer EJ, Nenke MA, Falhammar H, Torpy DJ. 2023. Corticosteroid-binding globulin (CBG): spatiotemporal distribution of cortisol in sepsis. *Trends Endocrinol Metab*. **34**:181–190. https://doi.org/10.1016/j.tem.2023.01.002.

Lee JH et al. 2025. Mass spectrometric detection of neutrophil elastase cleaved corticosteroid binding globulin and its association with Asn347 site glycosylation, in septic shock patients. *Clin Chim Acta*. **567**:120108. https://doi.org/10.1016/j.cca.2024.120108.

Lewis JG, Elder PA. 2014. The reactive Centre loop of corticosteroid-binding globulin (CBG) is a protease target for cortisol release. *Mol Cell Endocrinol*. **384**:96–101. https://doi.org/10.1016/j.mce.2014.01.005.

Lin YH, Zhu J, Meijer S, Franc V, Heck AJR. 2019. Glycoproteogenomics: a frequent gene polymorphism affects the glycosylation pattern of the human serum Fetuin/alpha-2-HS-glycoprotein. *Mol Cell Proteomics*. **18**:1479–1490. https://doi.org/10.1074/mcp.RA119.001411.

Meyer EJ et al. 2019. Total and high-affinity corticosteroid-binding globulin depletion in septic shock is associated with mortality. *Clin Endocrinol*. **90**:232–240. https://doi.org/10.1111/cen.13844.

Meyer EJ et al. 2020. Pyrexia and acidosis act independently of neutrophil elastase reactive center loop cleavage to effect cortisol release from corticosteroid-binding globulin. *Protein Sci*. **29**:2495–2509. https://doi.org/10.1002/pro.3982.

Meyer EJ et al. 2022. Corticosteroid-binding globulin deficiency independently predicts mortality in septic shock. *J Clin Endocrinol Metab*. **107**:1636–1646. https://doi.org/10.1210/clinem/dgac035.

Nenke MA et al. 2015. Depletion of high-affinity corticosteroid-binding globulin corresponds to illness severity in sepsis and septic shock; clinical implications. *Clin Endocrinol*. **82**:801–807. https://doi.org/10.1111/cen.12680.

Pemberton PA, Stein PE, Pepys MB, Potter JM, Carrell RW. 1988. Hormone binding globulins undergo serpin conformational change in inflammation. *Nature*. **336**:257–258. https://doi.org/10.1038/336257a0.

Perez-Riverol Y et al. 2022. The PRIDE database resources in 2022: a hub for mass spectrometry-based proteomics evidences. *Nucleic Acids Res*. **50**:D543–D552. https://doi.org/10.1093/nar/gkab1038.

Perogamvros I, Ray DW, Trainer PJ. 2012. Regulation of cortisol bioavailability—effects on hormone measurement and action. *Nat Rev Endocrinol*. **8**:717–727. https://doi.org/10.1038/nrendo.2012.134.

Piagnerelli M et al. 2005. Rapid alterations in transferrin sialylation during sepsis. *Shock*. **24**:48–52. https://doi.org/10.1097/01.shk.0000168524.20588.67.

Rebecchi KR, Wenke JL, Go EP, Desaire H. 2009. Label-free quantitation: a new glycoproteomics approach. *J Am Soc Mass Spectrom*. **20**:1048–1059. https://doi.org/10.1016/j.jasms.2009.01.013.

Reily C, Stewart TJ, Renfrow MB, Novak J. 2019. Glycosylation in health and disease. *Nat Rev Nephrol*. **15**:346–366. https://doi.org/10.1038/s41581-019-0129-4.

Rudd KE et al. 2020. Global, regional, and national sepsis incidence and mortality, 1990-2017: analysis for the global burden of disease study. *Lancet*. **395**:200–211. https://doi.org/10.1016/S0140-6736(19)32989-7.

Sackstein R. 2022. Glycans in acquired human diseases. In: Varki A, et al., editors. Cold Spring Harbor (NY): Essentials of Glycobiology. pp. 615–630.

Schilling B et al. 2012. Platform-independent and label-free quantitation of proteomic data using MS1 extracted ion chromatograms in skyline: application to protein acetylation and phosphorylation. *Mol Cell Proteomics*. **11**:202–214. https://doi.org/10.1074/mcp.M112.017707.

Siiteri PK et al. 1982. The serum transport of steroid hormones. *Recent Prog Horm Res*. **38**:457–510. https://doi.org/10.1016/b978-0-12-571138-8.50016-0.

Simard M et al. 2014. Pseudomonas aeruginosa elastase disrupts the cortisol-binding activity of corticosteroid-binding globulin. *Endocrinology*. **155**:2900–2908. https://doi.org/10.1210/en.2014-1055.

Simard M, Underhill C, Hammond GL. 2018. Functional implications of corticosteroid-binding globulin N-glycosylation. *J Mol Endocrinol*. **60**:71–84. https://doi.org/10.1530/JME-17-0234.

Singer M et al. 2016. The third international consensus definitions for sepsis and septic shock (Sepsis-3). *JAMA*. **315**:801–810. https://doi.org/10.1001/jama.2016.0287.

Stavenhagen K et al. 2018. N- and O-glycosylation analysis of human C1-inhibitor reveals extensive mucin-type O-glycosylation. *Mol Cell Proteomics*. **17**:1225–1238. https://doi.org/10.1074/mcp.RA117.000240.

Sumer-Bayraktar Z et al. 2011. N-glycans modulate the function of human corticosteroid-binding globulin. *Mol Cell Proteomics*. **10**:M111.009100. https://doi.org/10.1074/mcp.M111.009100.

Sumer-Bayraktar Z et al. 2016. Asn347 glycosylation of corticosteroid-binding globulin fine-tunes the host immune response by modulating proteolysis by Pseudomonas aeruginosa and neutrophil elastase. *J Biol Chem*. **291**:17727–17742. https://doi.org/10.1074/jbc.M116.735258.

Thaysen-Andersen M et al. 2015. Human neutrophils secrete bioactive paucimannosidic proteins from azurophilic granules into pathogen-infected sputum. *J Biol Chem*. **290**:8789–8802. https://doi.org/10.1074/jbc.M114.631622.

Tian W et al. 2021. O-glycosylation pattern of the SARS-CoV-2 spike protein reveals an "O-follow-N" rule. *Cell Res*. **31**:1123–1125. https://doi.org/10.1038/s41422-021-00545-2.

Tjondro HC et al. 2020. Hyper-truncated Asn355- and Asn391-glycans modulate the activity of neutrophil granule myeloperoxidase. *J Biol Chem*. **296**:100144. https://doi.org/10.1074/jbc.RA120.016342.

Uhlén M et al. 2015. Tissue-based map of the human proteome. *Science*. **347**:1260419. https://doi.org/10.1126/science.1260419.

Wei L et al. 2023. Elucidation of N-/O-glycosylation and site-specific mapping of sialic acid linkage isomers of SARS-CoV-2 human receptor angiotensin-converting enzyme 2. *Analyst*. **148**:5002–5011. https://doi.org/10.1039/D3AN01079A.

Westphal U. 1986. Corticosteroid-binding globulin (CBG). In: Gross F, Grumbach MM, Labhart A, Lipsett MB, Mann T, Samuels LT, Zander J, editors. *Steroid-protein interactions II*. Monographs on Endocrinology, Vol. **27**, Berlin, Heidelberg: Springer pp. 53–137. https://doi.org/10.1007/978-3-642-82486-9_5.

Yang W, Ao M, Hu Y, Li QK, Zhang H. 2018. Mapping the O-glycoproteome using site-specific extraction of O-linked

glycopeptides (EXoO). *Mol Syst Biol*. **14**:e8486. https://doi.org/10.15252/msb.20188486.
Zhang YY, Ning BT. 2021. Signaling pathways and intervention therapies in sepsis. *Signal Transduct Target Ther*. **6**:407. https://doi.org/10.1038/s41392-021-00816-9.
Zouaghi H et al. 1985. Total and unbound cortisol-, progesterone-, oestrone- and transcortin-binding activities in sera from patients with myocardial infarction: evidence for differential responses of good and bad prognostic cases. *Eur J Clin Investig*. **15**:365–370. https://doi.org/10.1111/j.1365-2362.1985.tb00286.x.

Glycobiology, 2025, 35, cwaf013
https://doi.org/10.1093/glycob/cwaf013
Original Article